

Cite this: *Biomater. Sci.*, 2017, 5, 1603

## Intracellular accumulation and immunological responses of lipid modified magnetic iron nanoparticles in mouse antigen processing cells

Chenmeng Qiao, <sup>a,b</sup> Jun Yang, <sup>b</sup> Lei Chen,<sup>\*c</sup> Jie Weng<sup>\*a</sup> and Xin Zhang<sup>\*b</sup>

Understanding the effects of magnetic iron nanoparticles (MINPs) on the immune response is vitally important for biomedical applications such as cancer therapy, disease diagnosis and novel cancer imaging. In this study, lipid modified MINPs were designed and prepared by introducing the neutral lipid DSPE-PEG or the zwitterionic lipid DSPE-PCB into hydrophobic MINPs through hydrophobic interaction (L-MINPs and ZL-MINPs, respectively). The effect of L-MINPs and ZL-MINPs on the intracellular accumulation and immune responses of three kinds of antigen processing cells was examined. The results indicated that the high cellular uptake efficiency of surface coated MINPs was strongly related to the nature of the coating lipid, with the zwitterionic lipid being more effective than PEGylated ones. Besides, the results from flow cytometry (FCM), confocal laser scanning microscopy (CLSM) and Prussian blue staining demonstrated a time- and concentration-dependent MINP internalization. The uptake of zwitterionic lipid modified MINPs (ZL-MINPs) induced very low cytotoxicity and a strong mixed Th1/Th2 type immune response. L-MINPs could induce a strong increase in pro-inflammatory cytokines with a slight secretion of Th2 cytokines. Besides, no IL-10 was observed in both groups, indicating that MINPs with lipid modification were absence of immunosuppression. In conclusion, this study addresses an important implication of the lipid type and Fe concentration on the immune stimulation of cells and supports the potential for further development of biomedical applications.

Received 24th March 2017,  
Accepted 29th April 2017

DOI: 10.1039/c7bm00244k

rsc.li/biomaterials-science

<sup>a</sup>Key Laboratory of Advanced Technologies of Materials, Ministry of Education, School of Materials Science and Engineering, Southwest Jiaotong University, Chengdu 610031, PR China. E-mail: jweng@swjtu.cn; Fax: +86 28 87601371; Tel: +86 28 87601371

<sup>b</sup>State Key Laboratory of Biochemical Engineering, Institute of Process Engineering, Chinese Academy of Sciences, Beijing 100190, PR China. E-mail: xzhang@ipe.ac.cn; Fax: +86 10 82544853; Tel: +86 10 82544853

<sup>c</sup>Department of Obstetrics and Gynecology, Navy General Hospital of People Liberation Army, Beijing 100048, PR China. E-mail: chenleis@mail.tsinghua.edu.cn; Tel: +11-86 18600310261

## Introduction

Nanoparticles have been investigated in various fields of biomedical research for decades due to their unique electronic, optical and magnetic properties.<sup>1–3</sup> Among the different types of nanoparticles, magnetic iron oxide nanoparticles (MINPs) with extensive shape and size control, tuneable magnetism and biocompatibility have attracted a great deal of attention



Chenmeng Qiao

Chenmeng Qiao is currently pursuing her PhD in materials science and engineering at the Institute of Process Engineering (Chinese Academy of Sciences) in the group of Prof. Xin Zhang. Her thesis work focuses on the development of a nucleic acid vaccine adjuvant and the MRI visualization of drug delivery systems.



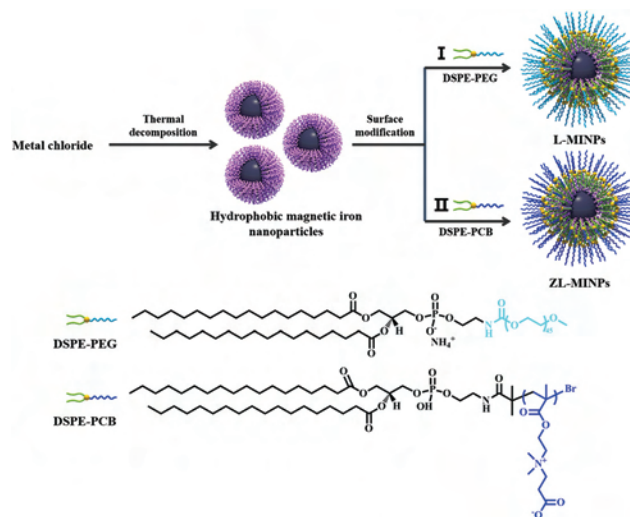
Jun Yang

Jun Yang received her PhD from and did postdoctoral work at Zhejiang University (China). She is currently an associate professor at the Institute of Process Engineering (Chinese Academy of Sciences), working with Prof. Xin Zhang to research biomaterials, drug delivery and vaccine.

for drug delivery, cancer imaging and immune activation applications.<sup>4–6</sup> Generally, MINPs consist of two segments: (I) a hydrophobic magnetic iron oxide core and (II) the outer coating which is utilized to improve their solubility, biocompatibility and colloidal stability, such as fatty acids, polysaccharides, polymers or lipids.<sup>7–9</sup> It is necessary to modify MINPs with coating due to their hydrophobic surfaces with large surface-to-volume ratios and propensity to agglomerate.<sup>10</sup>

The first encounter and the physical barrier between biological systems and magnetic iron oxide cores is the surface coating. Thus, the behaviour of MINPs in a variety of applications is greatly affected by the properties of the surface coatings.<sup>11–13</sup> For instance, Hu *et al.* introduced neutral lipids 1,2-distearoyl-*sn*-glycero-3-phosphor-ethanolamine-*N*-[methoxy(polyethyleneglycol)-2000] (DSPE-PEG2000) into magnetic nanoparticles to improve the performance of NPs.<sup>8</sup> The obtained DSPE-PEG coated nanoparticles possessed a fine serum stability and a long blood circulation lifetime which were probably due to the capability of DSPE-PEG coating to resist non-specific protein absorption.<sup>14</sup> The zeta potential or lipid type could also alter the behaviour of modified MINPs. Using multiple emulsions, Akbaba *et al.* developed cationic lipid coated magnetic nanoparticles with an appropriate particle size and surface zeta potential for drug or nucleic acid delivery.<sup>15</sup> Moreover, for a full understanding, the influence of different surface coatings on cells was also tested by Xu and his colleagues.<sup>16</sup> Nevertheless, the immunological effects of lipid modified MINPs are seldom evaluated.

In this paper, given the importance of macrophages and APCs in the immune response of the organism to nanoparticles, the effect of DSPE-PEG modified and DSPE-PCB modified MINPs on these cells was evaluated, namely their capacity to uptake into cells and to elicit the immune response (Scheme 1). The obtained results showed that the studied



**Scheme 1** The preparation of neutral lipid modified magnetic iron nanoparticles (L-MINPs) and zwitterionic lipid modified magnetic iron nanoparticles (ZL-MINPs).

DSPE-PEG modified and DSPE-PCB modified MINPs had a high uptake efficiency and could induce the secretion of cytokines in a time- and concentration-dependent manner. This lipid type showed a significant effect on the type of immune response which is related to the type of secret cytokine.

## Experimental section

### Materials

$\text{FeCl}_3 \cdot 6\text{H}_2\text{O}$ ,  $\text{CuCl}_2 \cdot 2\text{H}_2\text{O}$ , ethanol, hexane, chloroform, and *N,N*-dimethylformamide (DMF) were all purchased from Beijing Chemicals (Beijing, China). 1-Octadecene,



**Lei Chen**

*Lei Chen received her PhD in medicine from the Fourth Military Medical University and did postdoctoral work at Tsinghua University (China). She is currently a director of Obstetrics and Gynecology, chief physician. Her study focuses on the key technologies and drug resistance of gene therapy targeted delivery.*



**Jie Weng**

*Jie Weng received his BS (1983) in solid state physics from Sichuan University and his PhD (1995) from Leiden University in biological materials (the Netherlands). He is a Professor at the Key Laboratory of Advanced Technologies of Materials (MOE), School of Materials Science and Engineering, Southwest Jiaotong University. Prof. Jie Weng is also a member of the editorial board of The Scientific World Journal in biomaterials subject area, an expert reviewer of Acta Biomater., J. Bone Miner. Res., J. Med. Soc., Surf. Coat. Technol., and Mater. Lett., as well as a director of the biological material branch, Institute of Chinese Materials & Institute of Chinese Biomedical Engineering.*

$\beta$ -propiolactone (98%), copper bromide (98%), 2-bromo-2-methylpropionyl bromide and 2-(*N,N'*-dimethylamino) ethyl methacrylate (DMAEMA, 98%) were obtained from J&K Scientific Ltd (Shanghai, China). Sodium oleate (95%), oleic acid (90%), 1-octadecene (95%), *N,N,N',N',N''*-pentamethyldiethylenetriamine (PMDETA, 99%), triethylamine (TEA, 99%), iron assay kit (MAK025), 3-[4,5-dimethylthiazol-2-yl]-2,5-diphenyltetrazolium bromide (MTT) and deuterium reagent were purchased from Sigma-Aldrich (St Louis, Missouri, USA). DSPE-PEG was purchased from Advanced Vehicle Technology Ltd, Co. (Shanghai, China). Roswell Park Memorial Institute (RPMI) 1640, penicillin (10 000 U mL<sup>-1</sup>), streptomycin (10 mg mL<sup>-1</sup>), trypsin-EDTA and fetal bovine serum (FBS) were purchased from Invitrogen (Carlsbad, CA, USA). 4',6-Diamidino-2-phenylindole dihydrochloride (DAPI) and Prussian blue staining kit were obtained from Solarbio Science & Technology Co., Ltd (Beijing, China). Cy5 dye was purchased from Fanbo Biochemicals Co., Ltd (Beijing, China). LysoTracker Green was purchased from Invitrogen. ProcartaPlex™ multiplex immunoassays panels (EPX060-20931-901, Essential Th1/Th2 cytokines panel), mouse IL-2 simplex (EPX01A-20601-901), mouse IL-10 (EPX01A-20614-901) were obtained from eBioscience (CA, USA). All the reagents were of analytical grade and used without further purification. High-purity water (Milli-Q Integral) with a conductivity of 18 M $\Omega$  cm<sup>-1</sup> was used for the preparation of all aqueous solutions.

### Synthesis of DSPE-PCB

DSPE-PCB was synthesized according to the method reported by our group using an atom transfer radical polymerization (ATRP).<sup>17</sup>

### Preparation of magnetic iron nanoparticles (MINPs)

The magnetic iron nanoparticles (MINPs) were synthesized by high temperature thermal decomposition as reported in our previous work.<sup>18</sup> In brief, 5.4 g of FeCl<sub>3</sub>·6H<sub>2</sub>O and 18.25 g of sodium oleate were dissolved in a mixture of 40 mL ethanol, 30 mL distilled water and 70 mL hexane. The mixed solution

was reacted by refluxing at 70 °C for 4 h. The impurities and the iron-oleate complexes within the upper organic solution were washed three times with 30 mL distilled water in a separating funnel. The iron-oleate complex was obtained after the removal of remaining hexane. Then 3.6 g of the received iron-oleate complex and 0.57 g of oleic acid were dissolved in 20 g of 1-octadecene at room temperature. The reaction mixture was heated to 320 °C with a constant heating rate of 10 °C per 3 min, and kept at that temperature for 30 min. Then the initial transparent solution became turbid and brownish black. The resulting solution was cooled to room temperature, and ethanol was added to the solution to precipitate the oleic acid coated iron oxide nanoparticles. The nanoparticles were separated by centrifugation (5000 rpm for 10 min  $\times$  3 times) to yield a dark-brown precipitate. Finally, the product was stored as a solution of known concentration in hexane in a fridge.

### Preparation of lipid modified MINPs (L-MINPs) and zwitterionic lipid modified MINPs (ZL-MINPs)

The lipid modified MINPs (L-MINPs) were prepared by thin film dispersion as follows.<sup>17</sup> In brief, magnetic iron nanoparticles and DSPE-PEG with a mass ratio of 1:2 were dissolved in chloroform, and then the organic phase was removed at 55 °C on a rotary evaporator to obtain a thin lipid film. Vacuum was used to remove the residual solvents. The lipid films were finally hydrated in 5 mL phosphate buffered saline (0.01 M PBS, pH 7.4) under sonication for 30 min to obtain L-MINP solution. The zwitterionic lipid modified MINPs (ZL-MINPs) were prepared by the same method as above, with only DSPE-PEG instead of DSPE-PCB. The Fe concentration of L-MINPs and ZL-MINPs was tested with an iron assay kit according to the protocol.

### Preparation of Cy5 labelled lipid modified MINPs (L-MINPs) and Cy5 labelled zwitterionic lipid modified MINPs (ZL-MINPs)

Cy5 labelled L-MINPs were prepared according to the mentioned method with slight changes. Briefly, the fat-soluble dye Cy5, magnetic iron nanoparticles and DSPE-PEG with a mass ratio of 0.01:1:2 were dissolved in chloroform, and then the organic phase was removed at 55 °C on a rotary evaporator to obtain a thin lipid film. Vacuum was used to remove the residual solvents. The lipid films were finally hydrated in 5 mL phosphate buffered saline (0.01 M PBS, pH 7.4) under sonication for 30 min to obtain Cy5 labelled L-MINP solution. Cy5 labelled L-MINPs and ZL-MINPs were filtered using Amicon® cut-off filters (2 kDa) at 10 000 rpm for 10 min and diluted with 5 mL phosphate buffered saline (PBS 0.01 M, pH 7.4). The Cy5 labelled zwitterionic lipid modified MINPs (ZL-MINPs) were prepared by the same method as above, with only DSPE-PEG instead of DSPE-PCB.

### Physicochemical characterization

The hydrodynamic diameters and zeta potentials of lipid modified MINPs (L-MINPs) and zwitterionic lipid modified MINPs (ZL-MINPs) were measured by using a dynamic light



Xin Zhang

*Xin Zhang received her MS (2001) in polymer materials from Tianjin University and PhD (2008) in life science from the University of Strasbourg (France). She is a Professor at the Institute of Process Engineering, Chinese Academy of Sciences. Prof. Xin Zhang is a member of the American Chemical Society, and a committee member of Chinese Society for Biomaterials as well as a committee member of Chinese Society for Biomedical Engineering.*

scattering (DLS) instrument (Malvern Nano ZS). The morphologies of the magnetic iron nanoparticles, lipid modified MINPs (L-MINPs) and zwitterionic lipid modified MINPs (ZL-MINPs) were determined by transmission electron microscopy (H-7650 TEM, Japan). These NPs were dripped onto 200 mesh copper grids coated with carbon. The Cy5 labelled L-MINPs and ZL-MINPs were added in DMEM containing 10% FBS at 37 °C with gentle shaking at designated time points of 1, 2, 4, 8, 12, 24, 36 and 48 h. The serum stability of L-MINPs and ZL-MINPs was evaluated by measuring the average size with DLS and fluorescence with a microplate spectrophotometer (the absorbance at  $\lambda_{em} = 646$  nm and  $\lambda_{ex} = 664$  nm) in the triple test. The fluorescence intensity was normalized to the maximum emission of Cy5 labelled L-MINPs and ZL-MINPs at 0 h.

### Cell culture

RAW264.7 (one kind of macrophage) from the Chinese Academy of Medical Sciences was maintained in DMEM supplemented with 10% FBS and 1% v/v penicillin/streptomycin at 37 °C with 5% CO<sub>2</sub>. DC2.4 (one kind of dendritic cell) and J774 (one kind of macrophage) cells from the Chinese Academy of Medical Sciences tumour cell bank were maintained in RPMI 1640 supplemented with 10% FBS and 1% v/v penicillin/streptomycin at 37 °C with 5% CO<sub>2</sub>. All these three cell lines are derived from mice.

### Cytotoxicity measurement

The cytotoxicity of the prepared MINPs was evaluated through the MTT assay against these three kinds of cells. Briefly, 100  $\mu$ L of cell suspension ( $5 \times 10^4$  cells per mL) were seeded on 96-well plates. After the cells were incubated with various NPs for 24 h and 48 h, 20  $\mu$ L MTT solution ( $5$  mg mL<sup>-1</sup> in sterile  $1 \times$  PBS) was added to each well, and incubated for 3 h at 37 °C. Finally, the absorbance was measured at 490 nm using a microplate reader. The percentage of cell viability was determined by comparing cells treated with various NPs with the untreated control cells.

### Flow cytometry measurement

The cellular uptake of MINPs was evaluated by flow cytometry. Briefly, the cells were seeded in 24-well plates at a density of  $1 \times 10^5$  cells per mL in 500  $\mu$ L of culture medium and allowed to adhere for 24 h. The concentration and time-dependent cellular uptake of L-MINPs and ZL-MINPs were conducted by incubating these MINPs with three cell lines, RAW264.7, DC2.4 and J774 cells. After a certain period time of co-culture, the cells were rinsed with  $1 \times$  PBS for three times, trypsinized and harvested in PBS. Then the samples were assessed by BD Calibur flow cytometry to determine the fluorescence intensity of Cy5 loaded within L-MINPs or ZL-MINPs (red fluorescence).

### Confocal laser scanning microscopy (CLSM) analysis

The intracellular location of MINPs was investigated using a confocal laser scanning microscope (CLSM). Briefly,  $1 \times 10^5$  cells were plated into Petri dishes and allowed to attach

overnight. The MINPs were then added into each dish and incubated for 3 h (Fe concentration:  $0.1$  mg mL<sup>-1</sup>). Then the cells were washed three times with  $1 \times$  PBS and incubated with LysoTracker Green dye solution for 20 min at 37 °C. When the time was up, cells were washed with  $1 \times$  PBS again and fixed subsequently in 4% paraformaldehyde for 10 min at room temperature. Finally, cells were rinsed with  $1 \times$  PBS for three times and the nuclei were stained with DAPI for 10 min at room temperature. The fluorescence was observed using a Zeiss LSM780 confocal microscope.

### Prussian blue staining

DC2.4 cells were seeded in cell culture dishes at a density of  $1 \times 10^5$  cells per mL and cultured overnight. The cells were incubated with of fresh culture medium, L-MINPs or ZL-MINPs (Fe concentration:  $0.1$  mg mL<sup>-1</sup>), respectively. After 24 h incubation, cells were stained with Prussian blue according to the instructions.

### Cytokines expression

The secretion of cytokines was assayed after incubation with RAW264.7, DC2.4 and J774, respectively. In detail, cells were plated into a 24-well plate overnight, and then were incubated with the prepared nanoparticles for 24 h. After that the supernatant was collected and detected with ProcartaPlex multiplex immunoassays panels. The levels of cytokines were detected by using the Luminex 100/200 System (Thermo Fisher Scientific, Pittsburgh, PA, USA).

### Statistical analysis

All data from three independent experiments were expressed as means  $\pm$  standard deviations (SD). Differences were analysed by using one-factor analysis of variance (ANOVA), and were considered significant when  $p < 0.05$ .

## Results and discussion

### Synthesis and characterization of a DSPE-PCB polymer

Firstly, we prepared the CB monomer by conjugating DMAEMA and  $\beta$ -propiolactone through the ring open reaction. <sup>1</sup>H NMR spectra recorded for CB are shown in Fig. 1A. <sup>1</sup>H NMR (600 MHz, D<sub>2</sub>O,  $\delta$ ): 6.06 (s, 1H, -CH=CCH<sub>3</sub>-), 5.85 (s, 1H, -CH=CCH<sub>3</sub>-), 4.58 (m, 2H, -OCH<sub>2</sub>CH<sub>2</sub>N-), 3.70 (m, 2H, -OCH<sub>2</sub>CH<sub>2</sub>N-), 3.59 (t, 2H, -NCH<sub>2</sub>CH<sub>2</sub>COO-), 3.10 (s, 6H, -NCH<sub>3</sub>CH<sub>3</sub>-), 2.64 (t, 2H, -NCH<sub>2</sub>CH<sub>2</sub>COO-), 1.84 (s, 3H, CH<sub>2</sub>=CCH<sub>3</sub>).

The ATRP initiator (DSPE-Br) was obtained through the esterification reaction of the terminal amino group of the DSPE with 2-bromoisoobutryl bromide. The final structure of DSPE-Br was confirmed by <sup>1</sup>H NMR spectra (Fig. 1B). <sup>1</sup>H NMR (600 MHz, CDCl<sub>3</sub>):  $\delta = 5.20$ : -OCHCH<sub>2</sub>O-P-;  $\delta = 4.40$ : -CH<sub>2</sub>COOCH<sub>2</sub>-;  $\delta = 4.18$ : -P-OCH<sub>2</sub>CH<sub>2</sub>-;  $\delta = 3.98$ : -P-OCH<sub>2</sub>CH-;  $\delta = 3.44$ : -OCH<sub>2</sub>CH<sub>2</sub>N-;  $\delta = 2.25$ : -COCH<sub>2</sub>CH<sub>2</sub>-;  $\delta = 1.86$ : -BrCCH<sub>3</sub>CH<sub>3</sub>;  $\delta = 1.58$ : -COCH<sub>2</sub>CH<sub>2</sub>-;  $\delta = 1.23$ : -(CH<sub>2</sub>)<sub>14</sub>-;  $\delta = 0.88$ : -CH<sub>2</sub>CH<sub>3</sub>.

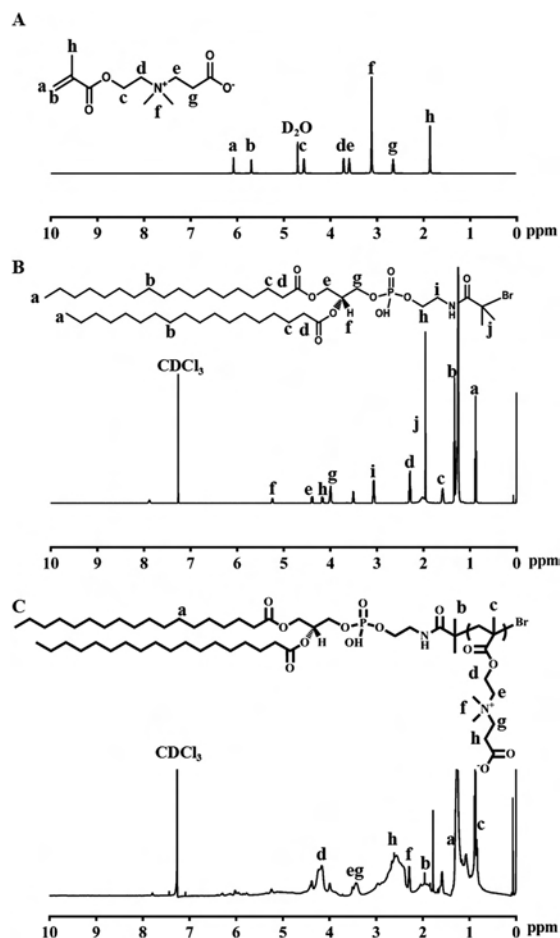


Fig. 1  $^1\text{H}$  NMR spectra recorded for the (A) CB monomer; (B) DSPE-Br initiator and (C) DSPE-PCB polymer.

Finally, DSPE-PCB polymers were synthesized by the ATRP of the DSPE-Br initiator and the CB monomer with the CuBr/PMDETA as the catalyst system. The structure of DSPE-PCB was confirmed by the  $^1\text{H}$  NMR spectrum, and the degree of polymerization of PCB was 20 (Fig. 1C).  $^1\text{H}$  NMR (600 MHz,  $\text{CDCl}_3$ ):  $\delta = 4.10$ :  $-\text{OCH}_2\text{CH}_2\text{N}-$ ;  $\delta = 3.0-4.8$ :  $-\text{OCH}_2\text{CH}_2\text{NCH}_2\text{CH}_2-$ ;  $\delta = 2.60$ :  $-\text{NCH}_2\text{CH}_2\text{COO}-$ ;  $\delta = 2.25$ :  $-\text{NCH}_3\text{CH}_3-$ ;  $\delta = 1.80$ :  $-\text{NHCOCCH}_3$ ;  $\delta = 1.20-1.28$ :  $-(\text{CH}_2)_{14}-\text{CH}_3$ ;  $\delta = 1.00$ :  $-\text{BrCH}_2\text{CCH}_3$ .

### Preparation and characterization of lipid modified magnetic iron nanoparticles (MINPs)

The magnetic iron nanoparticles were prepared by the thermal decomposition method (Scheme 1). As shown in Fig. 2A, the hydrophobic MINPs were monodispersed and had a spherical structure with diameters of around 10 nm. In order to obtain water-soluble MINPs, a two-lipid based polymer was utilized for surface modification. The dynamic light scattering (DLS) results showed that the modified MINPs had a similar diameter of around 40 nm due to the presence of lipids surrounding the metal core (Fig. 2B). The zeta potentials of each NP are  $-1.87$  mV and  $8.76$  mV, respectively (Fig. 2B insert). The TEM

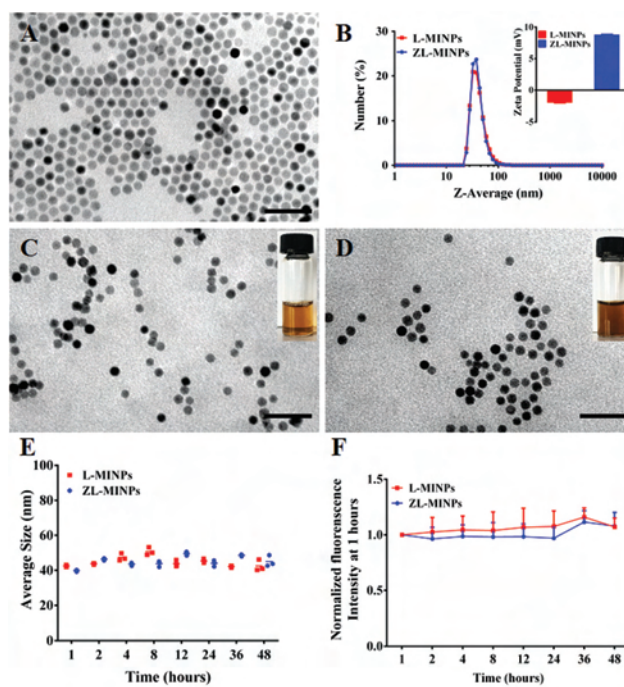


Fig. 2 The characterization of nanoparticles. (A) The TEM images of magnetic iron nanoparticles; (B) the hydrodynamic sizes and distribution of surface coated MINPs measured by DLS in PBS (0.01 M, pH 7.4), the insert image: the zeta potentials of surface coated MINPs measured by using a potential analyser in PBS (0.01 M, pH 7.4); (C) the TEM images of DSPE-PEG lipid modified MINPs (L-MINPs) and (D) DSPE-PCB lipid modified MINPs (ZL-MINPs), scale bar: 50 nm, insert maps: images of modified MINPs; (E) changes in particle average sizes of the surface coated MINPs after dispersion in DMEM containing 10% FBS followed over 48 h; (F) fluorescence stability of Cy5 labelled L-MINPs and Cy5 labelled ZL-MINPs dispersed in DMEM containing 10% FBS followed over 48 h. Fluorescence data are normalized to the maximum fluorescence intensity of MINPs measured 1 hour after dilution.

images confirmed the relatively high monodispersity of the modified MINPs (Fig. 2C and D).

The serum stability of MINPs was determined by following the changes of average size and fluorescence intensity in culture medium over time (Fig. 2E and F). L-MINPs and ZL-MINPs were dispersed in DMEM medium containing 10% fetal bovine serum (FBS) and sustained for 48 h. The average size of both MINPs was monitored by DLS at a predetermined time point. As shown in Fig. 2E, the diameter of L-MINPs and ZL-MINPs within culture medium barely changed during the incubation process. The minute changes in average sizes indicated that DSPE-PEG and DSPE-PCB could enhance the protein resistant adsorption ability of these MINPs in the presence of polyethyleneglycol or carboxyl groups.<sup>19</sup>

To further test the stability of these MINPs, a fat-soluble dye Cy5 was entrapped into the MINPs through the hydrophobic interaction. The fluorescence intensity of Cy5 within MINPs was measured after incubation with culture medium at different time intervals. The results showed that L-MINPs and ZL-MINPs had high serum stability which were in good agreement with the DLS results previously published (Fig. 1F).

### *In vitro* cytotoxicity of L-MINPs and ZL-MINPs

The cytotoxicity is essential for further application of these MINPs.<sup>20–22</sup> RAW264.7, J774 with strong phagocytosis ability and DC2.4 with the capability of presenting antigens were chosen as model cells to investigate the immune response of MINPs in this study.<sup>23,24</sup> The MTT assay was employed in three cell lines to measure the cytotoxicity of L-MINPs and ZL-MINPs. As shown in Fig. 3A and B, no appreciable toxicity was observed up to a very high concentration of 0.5 mg mL<sup>-1</sup> at 24 h. On prolonging the incubation time to 48 h, a slight cytotoxicity was observed at high concentration, which demonstrated that an increase of MINP dosage as well as incubation time led to higher cytotoxicity (Fig. 3C and D). Thus, the Fe concentration from 0.01 mg mL<sup>-1</sup> to 0.1 mg mL<sup>-1</sup> was used in the following experiments.

### The cellular uptake measurement by flow cytometry (FCM)

In order to investigate the influence of lipid type, the Fe concentration and incubation time on cellular uptake efficiency, flow cytometry was performed after incubation of three cell lines with MINPs modified with DSPE-PEG or DSPE-PCB for 3 h, 6 h, 12 h and 24 h. The Fe concentration ranged from 0.01 mg mL<sup>-1</sup> to 0.1 mg mL<sup>-1</sup>. As shown in Fig. 4, the mean fluorescence intensity (MFI) of three cells incubated with ZL-MINPs for 24 h was 3.1, 24 and 14.6 times higher than that with L-MINPs, respectively. These results indicated that ZL-MINPs were internalized more readily than L-MINPs. This was probably due to the unique characteristics of PCB molecules, which could facilitate the cellular uptake through an electrostatic interaction between positively charged quaternary amine groups and negatively charged cell membranes.<sup>17,25</sup>

The effect of the Fe concentration on cellular uptake was also studied in this experiment (Fig. 4). The fluorescence intensity of MINPs increased in a concentration-dependent pattern after incubation with L-MINPs and ZL-MINPs from 0.01 to 0.1 mg mL<sup>-1</sup>. Moreover, the time-dependent uptake of

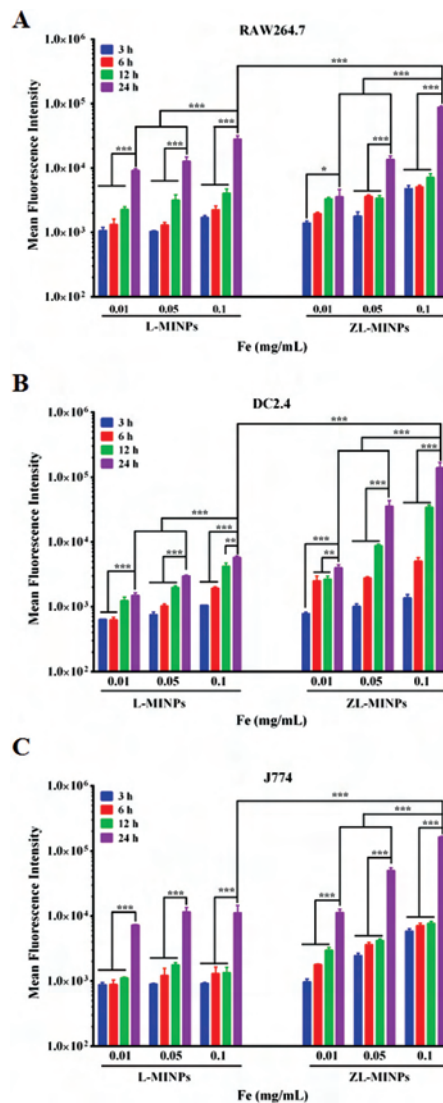


Fig. 4 Flow cytometry measurements of (A) RAW264.7, (B) DC2.4 and (C) J774 incubated with L-MINPs and ZL-MINPs at different Fe concentrations (mg mL<sup>-1</sup>) for 3 h, 6 h, 12 h and 24 h, respectively. \*: Differences between two corresponding groups under the line. \*:  $P < 0.05$ , \*\*:  $P < 0.01$ , \*\*\*:  $P < 0.001$ .

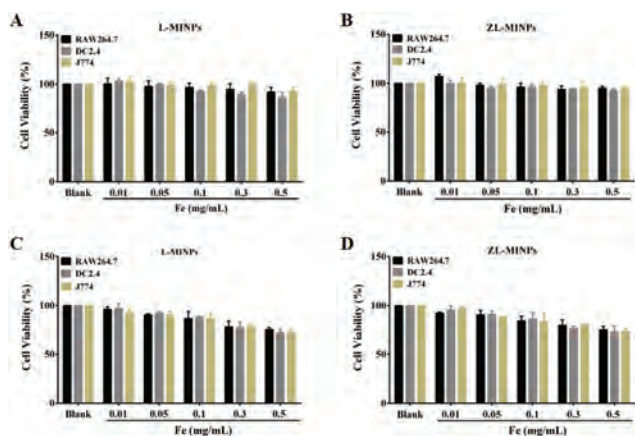
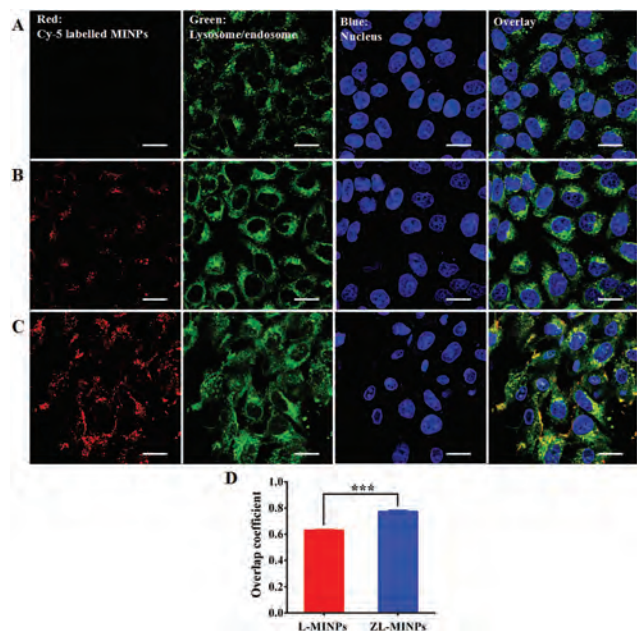


Fig. 3 The cytotoxicity of surface coated MINPs with various concentrations in RAW264.7, DC2.4, J774 cells after 24 h (A, B) and 48 h (C, D) incubation.

MINPs was examined by incubating cells with MINPs for 3 h, 6 h, 12 h and 24 h intervals, respectively. The results from flow cytometry demonstrated a constant cellular uptake of surface coated MINPs, which indicated that the uptake of surface coated MINPs was also in a time-dependent fashion. Collectively, the surface lipid coating showed an important effect on cellular uptake in a time- and concentration-dependent manner.

### The cellular uptake measurement by confocal laser scanning microscopy (CLSM)

The cellular uptake and intracellular distribution of these MINPs were further investigated by confocal laser scanning microscopy (CLSM) after 3 h of incubation (Fig. 5). DC2.4 cells



**Fig. 5** The cellular uptake of surface coated MINP loaded Cy5 assay by CLSM. CLSM images of MINPs (Cy5 dyes within MINPs, red fluorescence), lysosomes (stained with LysoTracker Green, green fluorescence), nucleus (stained with DAPI, blue fluorescence) and their overlay signals after incubation with (A) PBS, (B) L-MINPs and (C) ZL-MINPs for 3 h. The overlap coefficients of lysosomes and Cy5 were calculated by using Zen co-localization software (D) (scale bar: 20  $\mu$ m). Data in (D) are representative for 3 results in each group. \*: Differences between L-MINPs with ZL-MINPs groups. \*\*\*:  $P < 0.001$ .

were chosen as a model of cells. MINPs were loaded with Cy5 (red fluorescence dye). As shown in Fig. 5B, the L-MINP treated group exhibited an obvious red fluorescence around the nucleus, suggesting that the L-MINPs could endocytose into cells and reside in endosomes/lysosomes. Moreover, the cellular uptake of ZL-MINPs was significantly higher than L-MINPs (Fig. 5C). These results revealed that the surface coated MINPs could be taken up by cells successfully and ZL-MINPs were internalized more readily than L-MINPs, which were in agreement with the data shown in the flow cytometry experiment (Fig. 4).

### Prussian blue staining assay

Prussian blue staining was generally used to detect intracellular iron endocytosis.<sup>26–28</sup> The efficiency of endocytosis of these magnetic nanoparticles was further confirmed by the Prussian blue staining after incubating DC2.4 cells with L-MINPs and ZL-MINPs for 24 h, respectively. DC2.4 cells incubated with these magnetic nanoparticles were specifically labelled blue whereas DC2.4 cells without treatment showed no apparent blue. The results shown in Fig. 6 indicated that these magnetic nanoparticles could be taken up into the cytoplasm (Fig. 6). Consistent with previous results in Fig. 4 and 5, the cellular uptake of ZL-MINPs was much higher than the L-MINP group.

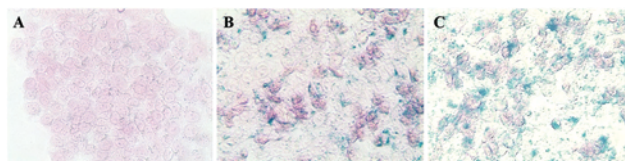


**Fig. 6** The cellular uptake of surface coated MINP assay by Prussian blue assay. DC2.4 cells were exposed to (A) PBS, (B) L-MINPs and (C) ZL-MINPs for 24 h, respectively. The cells were red stained and surface coated MINPs were blue stained in the cytoplasm (40 $\times$ ).

### The level of Th1/Th2 related cytokine detection

The secretion of cytokines plays a key role in modulating inflammatory and immunological mediators. In this study, the secretion of cytokines (IL-2, IL-5, IL-6, TNF- $\alpha$ , IFN- $\gamma$ , IL12p70, IL-4 and IL-10) was evaluated by ProcartaPlex multiplex immunoassay panels according to the manufacturer's instructions after 24 h of incubation with L-MINPs or ZL-MINPs at a Fe concentration from 0.01 mg mL<sup>-1</sup> to 0.1 mg mL<sup>-1</sup> (Fig. 7). Among these cytokines, IL-2, IL-12p70 and INF- $\gamma$  were typical T-helper 1 (Th1) type cytokines that were mainly associated with cellular immunity,<sup>29–32</sup> while IL-4 and IL-5 were reported as Th2 type cytokines, which were related to humoral immunity.<sup>31</sup> In addition, IL-10, one of the typical cytokines closely related to regulatory T cells (Treg cells), was also taken into consideration.<sup>33</sup> Besides, IL-6 and TNF- $\alpha$  were important inflammatory cytokines for the immune system.<sup>34</sup>

As shown in Fig. 7A–C, the secretion of Th1 cytokines (IL-2, IFN- $\gamma$ , and TNF- $\alpha$ ) in cells treated with L-MINPs was barely observed, while an obvious concentration-dependent secretion was observed in the ZL-MINP treated group. It has been reported that IL-2, IFN- $\gamma$ , and TNF- $\alpha$  had a great influence on the immune reaction through the cell-mediated immune response. These data indicated that the zwitterionic lipid DSPE-PCB could alter the Th1 immune response, while the neutral lipid DSPE-PEG showed the absence of triggering Th1 related immune response. In addition, there was a significant increase in the formation/release of Th2 cytokines (IL-4, IL-5) by cells upon incubation with ZL-MINPs compared with the non-treated group or the L-MINP group (Fig. 7D and E). Interesting, there was no great change in the secretion of IL-10, typical cytokines related to immune suppression (Fig. 7F). It had been clarified that Treg cells made a great difference in the immune suppression activity. It also made a contribution to the mechanism of organism tolerance and was important for the regulation of innate immunity. Inflammatory responses were closely related to the secretion of IL-6 and TNF- $\alpha$ . As shown in Fig. 7G and H, these two cytokines were secreted in a concentration-dependent manner. All these results suggested that the surface lipid coating had an important effect on immune responses according to the nature of surface coatings and in a concentration-dependent way. It could induce a Th1/Th2 pattern immune response without eliciting immunosuppression, also with the assistance of inflammation.

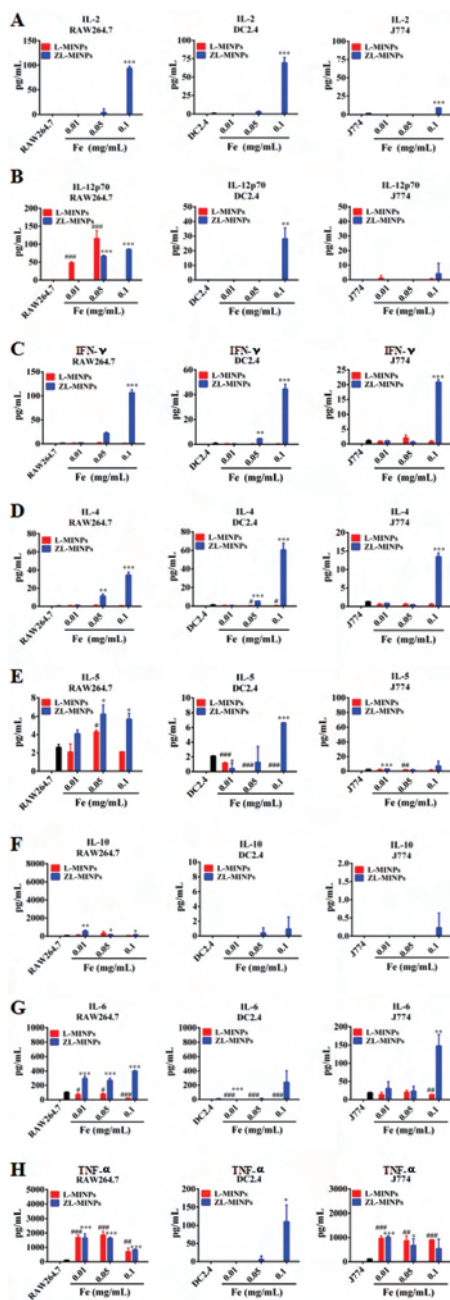


Fig. 7 Cytokine secretion from RAW264.7, DC2.4 and J774 cells with different MINPs at 0.01, 0.05 and 0.1 mg mL<sup>-1</sup> (Fe concentration) after 24 h. Bars represent the medium production of (A) IL-2, (B) IL12p70, (C) IFN- $\gamma$ , (D) IL-4, (E) IL-5, (F) IL-10, (G) IL-6 and (H) TNF- $\alpha$  with or without modified MINPs. The Wilcoxon test was used for statistical analysis. #: Differences between no treatment groups with L-MINPs groups, # $p$  < 0.05, ## $p$  < 0.01 and ### $p$  < 0.001; \*: differences between no treatment groups with ZL-MINPs groups. \* $p$  < 0.05, \*\* $p$  < 0.01 and \*\*\* $p$  < 0.001.

## Conclusions

In summary, the effect of different lipid coatings on the intracellular accumulation and the immune response of surface coated MINPs was studied. The surface coated MINPs were

developed by introducing a DSPE-PEG lipid or a DSPE-PCB lipid into hydrophobic MINPs through the hydrophobic interaction. The L-MINPs and ZL-MINPs were monodispersed in water with a mean diameter of about 40 nm. The modification of MINPs with both lipids showed no toxicity on cells at a Fe concentration from 0.01 to 0.1 mg mL<sup>-1</sup>. ZL-MINPs were internalized more readily than L-MINPs in a time- and concentration-dependent manner. It indicated that the DSPE-PCB lipid were more efficient to facilitate the cellular uptake through an electrostatic interaction between positively charged quaternary amine groups and negatively charged cell membranes. The cells treated with L-MINPs showed the absence of triggering Th1 related immune response, while the ZL-MINP group showed a significant enhancement in the secretion of Th2 cytokines (IL-4, IL-5) compared with the non-treated group or the L-MINP group. A Th1/Th2 pattern immune response without eliciting immunosuppression was also observed in the ZL-MINP treated group. The inflammatory response was elicited by secreting IL-6 and TNF- $\alpha$  in a concentration-dependent manner in all groups. Accordingly, the surface lipid coating has a great effect on intracellular accumulation as well as the immune response. Based on these data, it seems that useful information to select the surface coatings of MINPs for biological and biomedical applications is provided.

## Conflict of interest

The authors declare no competing financial interest.

## Acknowledgements

This work was financially supported by the National High Technology Research and Development Program (2016YFA0200303), the National Natural Science Foundation of China (No. 51573188, 31522023, 51373177, 51572228), the "Strategic Priority Research Program" of the Chinese Academy of Sciences (XDA09030301-3) and the Beijing Municipal Science & Technology Commission (No. Z161100002616015).

## Notes and references

- 1 P. Poizot, S. Laruelle, S. Grugeon, L. Dupont and J. M. Tarascon, *Nature*, 2000, **407**, 496–499.
- 2 R. Tietze, J. Zaloga, H. Unterweger, S. Lyer, R. P. Friedrich, C. Janko, M. Pottler, S. Durr and C. Alexiou, *Biochem. Biophys. Res. Commun.*, 2015, **468**, 463–470.
- 3 S. M. Ng, M. Koneswaran and R. Narayanaswamy, *RSC Adv.*, 2016, **6**, 21624–21661.
- 4 C. de Montferriand, L. Hu, I. Milosevic, V. Russier, D. Bonnin, L. Motte, A. Brioude and Y. Lalatonne, *Acta Biomater.*, 2013, **9**, 6150–6157.
- 5 A. G. Malyutin, H. Cheng, O. R. Sanchez-Felix, K. Carlson, B. D. Stein, P. V. Konarev, D. I. Svergun, B. Dragnea and

- L. M. Bronstein, *ACS Appl. Mater. Interfaces*, 2015, **7**, 12089–12098.
- 6 W. Wu, C. Z. Jiang and V. A. L. Roy, *Nanoscale*, 2016, **8**, 19421–19474.
- 7 S. Laurent, A. A. Saei, S. Behzadi, A. Panahifar and M. Mahmoudi, *Expert Opin. Drug Delivery*, 2014, **11**, 1449–1470.
- 8 B. B. Hu, M. Zeng, J. L. Chen, Z. Z. Zhang, X. N. Zhang, Z. M. Fan and X. Zhang, *Small*, 2016, **12**, 4707–4712.
- 9 M. Kim, S. W. Shin, C. W. Lim, J. Kim, S. H. Um and D. Kim, *Biomater. Sci.*, 2017, **5**, 305–312.
- 10 A. H. Lu, E. L. Salabas and F. Schuth, *Angew. Chem., Int. Ed.*, 2007, **46**, 1222–1244.
- 11 J. Sherwood, Y. Xu, K. Lovas, Y. Qin and Y. Bao, *J. Magn. Magn. Mater.*, 2017, **427**, 220–224.
- 12 A. A. Javidparvar, B. Ramezanzadeh and E. Ghasemi, *Prog. Org. Coat.*, 2016, **90**, 10–20.
- 13 S. Mondini, M. Leonzino, C. Drago, A. M. Ferretti, S. Usseglio, D. Maggioni, P. Tornese, B. Chini and A. Ponti, *Langmuir*, 2015, **31**, 7381–7390.
- 14 A. Verma and F. Stellacci, *Small*, 2010, **6**, 12–21.
- 15 H. Akbaba, U. Karagöz, Y. Selamet and A. G. Kantarcı, *J. Magn. Magn. Mater.*, 2017, **426**, 518–524.
- 16 Y. L. Xu, J. A. Sherwood, K. H. Lackey, Y. Qin and Y. P. Bao, *J. Appl. Toxicol.*, 2016, **36**, 543–553.
- 17 C. M. Qiao, J. D. Liu, J. Yang, Y. Li, J. Weng, Y. M. Shao and X. Zhang, *Biomaterials*, 2016, **85**, 1–17.
- 18 B. B. Hu, F. Y. Dai, Z. M. Fan, G. H. Ma, Q. W. Tang and X. Zhang, *Adv. Mater.*, 2015, **27**, 5499–5505.
- 19 R. Liu, Y. Li, Z. Zhang and X. Zhang, *Regener. Biomater.*, 2015, **2**, 125–133.
- 20 C. C. Hanot, Y. S. Choi, T. B. Anani, D. Soundarrajan and A. E. David, *Int. J. Mol. Sci.*, 2015, **17**, 54.
- 21 C. Costa, F. Brandao, M. J. Bessa, S. Costa, V. Valdiglesias, G. Kilic, N. Fernandez-Bertolez, P. Quaresma, E. Pereira, E. Pasaro, B. Laffon and J. P. Teixeira, *J. Appl. Toxicol.*, 2016, **36**, 361–372.
- 22 S. Ghasempour, M. A. Shokrgozar, R. Ghasempour and M. Alipour, *Exp. Toxicol. Pathol.*, 2015, **67**, 509–515.
- 23 J. K. Hsiao, H. H. Chu, Y. H. Wang, C. W. Lai, P. T. Choi, S. T. Hsieh, J. L. Wang and H. M. Liu, *NMR Biomed.*, 2008, **21**, 820–829.
- 24 V. Kodali, M. H. Littke, S. C. Tilton, J. G. Teeguarden, L. Shi, C. W. Frevert, W. Wang, J. G. Pounds and B. D. Thrall, *ACS Nano*, 2013, **7**, 6997–7010.
- 25 Y. Li, Q. Cheng, Q. Jiang, Y. Huang, H. Liu, Y. Zhao, W. Cao, G. Ma, F. Dai, X. Liang, Z. Liang and X. Zhang, *J. Controlled Release*, 2014, **176**, 104–114.
- 26 W. Liu, L. Nie, F. Li, Z. P. Aguilar, H. Xu, Y. Xiong, F. Fu and H. Xu, *Biomater. Sci.*, 2016, **4**, 159–166.
- 27 N. Peng, B. Wu, L. Wang, W. He, Z. Ai, X. Zhang, Y. Wang, L. Fan and Q. Ye, *Biomater. Sci.*, 2016, **4**, 1802–1813.
- 28 Y. Zeng, L. Wang, Z. Zhou, X. Wang, Y. Zhang, J. Wang, P. Mi, G. Liu and L. Zhou, *Biomater. Sci.*, 2016, **5**, 50–56.
- 29 T. D. Fernandez, J. R. Pearson, M. P. Leal, M. J. Torres, M. Blanca, C. Mayorga and X. Le Guevel, *Biomaterials*, 2015, **43**, 1–12.
- 30 K. R. Sigdel, L. Duan, Y. Wang, W. Hu, N. Wang, Q. Sun, Q. Liu, X. Liu, X. Hou, A. Cheng, G. Shi and Y. Zhang, *Mediators Inflammation*, 2016, **2016**, 4927530.
- 31 A. Elahi, Y. Sharma, S. Bashir and F. Khan, *J. Immunotoxicol.*, 2016, **13**, 335–348.
- 32 P. L. Mottram, D. Leong, B. Crimeen-Irwin, S. Gloster, S. D. Xiang, J. Meanger, R. Ghildyal, N. Vardaxis and M. Plebanski, *Mol. Pharmaceutics*, 2007, **4**, 73–84.
- 33 A. K. Abbas and A. H. Sharpe, *Nat. Immunol.*, 2005, **6**, 227–228.
- 34 K. Niikura, T. Matsunaga, T. Suzuki, S. Kobayashi, H. Yamaguchi, Y. Orba, A. Kawaguchi, H. Hasegawa, K. Kajino, T. Ninomiya, K. Ijiro and H. Sawa, *ACS Nano*, 2013, **7**, 3926–3938.